Programmed cell death 5 suppresses AKT-mediated cytoprotection of endothelium

Seung-Hyun Lee[a], Jaesung Seo[a], Soo-Yeon Park[a], Mi-Hyeon Jeong[a], Hyo-Kyoung Choi[b], Chan Joo Lee[c,1], Mi Jeong Kim[a], Garam Guk[a], SooYeon Lee[a], Hyewon Park[c], Jae-Wook Jeong[d], Chang Hoon Ha[e,2], Sungha Park[c,2], and Ho-Geun Yoon[a,2]

[a]Department of Biochemistry and Molecular Biology, Brain Korea 21 PLUS Project for Medical Sciences, Yonsei University College of Medicine, 03722 Seoul, Korea; [b]Division of Nutrition and Metabolism Research Group, Korea Food Research Institute, 13539 Gyeonggi-do, Korea; [c]Division of Cardiology, Department of Internal Medicine, Yonsei University College of Medicine, 03722 Seoul, Korea; [d]Department of Obstetrics, Gynecology, and Reproductive Biology, Michigan State University College of Human Medicine, MI 49503; and [e]Asan Institute for Life Sciences, Asan Medical Center, University of Ulsan College of Medicine, 13539 Seoul, Korea

Programmed cell death 5 (PDCD5) has been associated with human cancers as a regulator of cell death; however, the role of PDCD5 in the endothelium has not been revealed. Thus, we investigated whether PDCD5 regulates protein kinase B (PKB/AKT)-endothelial nitric oxide synthase (eNOS)–dependent signal transduction in the endothelium and affects atherosclerosis. Endothelial-specific PDCD5 knockout mice showed significantly reduced vascular remodeling compared with wild-type (WT) mice after partial carotid ligation. WT PDCD5 competitively inhibited interaction between histone deacetylase 3 (HDAC3) and AKT, but PDCD5[L6R], an HDAC3-binding–deficient mutant, did not. Knockdown of PDCD5 accelerated HDAC3–AKT interaction, AKT and eNOS phosphorylation, and nitric oxide (NO) production in human umbilical vein endothelial cells. Moreover, we found that serum PDCD5 levels reflect endothelial NO production and are correlated with diabetes mellitus, high-density lipoprotein cholesterol, and coronary calcium in human samples obtained from the cardiovascular high-risk cohort. Therefore, we conclude that PDCD5 is associated with endothelial dysfunction and may be a novel therapeutic target in atherosclerosis.

atherosclerosis | endothelium | PDCD5 | AKT | HDAC3

Vascular endothelial cells (ECs) line blood vessels and have a critical role in vascular homeostasis. Although the endothelium is a simple monolayer, it regulates various vessel properties such as integrity, tone, and immune cell recruitment (1). Nitric oxide (NO) is a potent vasodilator synthesized from L-arginine by NO synthase in ECs. NO regulates the vascular tone and blood flow by inhibiting vascular smooth muscle contraction. Dysfunctional endothelium with reduced NO levels stimulates the proliferation and migration of vascular smooth muscle cells (VSMCs). In addition, reduced NO levels promote atherosclerosis by increasing endothelial permeability, platelet aggregation, leukocyte adhesion, and cytokine generation (2).

Programmed cell death 5 (PDCD5) has a major role in cellular apoptosis. PDCD5 is expressed ubiquitously in various human tissues and has highly conserved sequences among species (3). It can dissociate the p53–Mdm2 interaction and activate the p53-dependent apoptotic pathway (4). PDCD5 can also accelerate the paraptosis (5) and autophagy (6, 7) pathways. Decreased PDCD5 expression is correlated with poor prognosis in various human cancers (8–10). Endothelial PDCD5 is up-regulated in the ischemic zone during cerebral ischemic/reperfusion injury (11), suggesting that enrichment of PDCD5 might affect endothelial integrity. A few studies have reported that PDCD5 protein is present in human serum and is increased in some autoimmune and inflammatory diseases (12, 13). The role of PDCD5 in the endothelium and the correlation between serum PDCD5 and atherosclerosis remain unclear, however.

Histone deacetylase 3 (HDAC3), a class I HDAC, can remove acetyl groups from lysine residues of histone and nonhistone proteins. It is a component of transcriptional repression complexes and presents mainly in the nucleus (14). A lack of HDAC3 leads to loss of heterochromatin and an increase in DNA double-strand breaks, which affects proliferation (15). HDAC3 is also present in the cytoplasm via a CRM1-mediated pathway and in the plasma membrane via a CRM1-independent pathway, suggesting that dynamic localization is a key regulator of HDAC3 function (14, 16). HDAC3 is an important factor in endothelial integrity and regulates protein kinase B (PKB/AKT) phosphorylation and activity (17).

In this study, in vivo analysis of endothelial-specific PDCD5 knockout (PDCD5cKO) mice demonstrated that PDCD5 is an essential factor for the progression of neointima hyperplasia. In vitro analysis demonstrated that PDCD5 inhibits AKT- endothelial nitric oxide synthase (eNOS) signaling by dissociating the HDAC3–AKT interaction, resulting in decreased NO production. We found that serum PDCD5 in human participants was significantly correlated with diabetes mellitus, coronary calcium burden, and high-density lipoprotein (HDL) cholesterol levels, which are markers of endothelial dysfunction. Taken together, our results strongly suggest that PDCD5 plays a significant role in endothelial dysfunction and could be a novel diagnostic marker and therapeutic target in atherosclerosis.

Significance

Programmed cell death 5 (PDCD5) plays a pivotal role in cellular apoptosis. Pathological relevance of PDCD5 is mostly found in human cancers; however, the role of PDCD5 in noncancerous diseases is not fully elucidated. Here we show that mice with endothelial PDCD5 deficiency have elevated serum nitric oxide levels and an atheroprotective effect in blood vessels. In addition, PDCD5 disrupts the HDAC3–protein kinase B (PKB/AKT) interaction and inhibits AKT-eNOS signaling and nitric oxide production in vivo and in vitro. Moreover, serum PDCD5 reflects vascular endothelial status, which is significantly correlated with cardiovascular risk. Our results demonstrate a mechanism of endothelial homeostasis and provide a potential therapeutic target for improving endothelial function.

Results

PDCD5 Plays a Crucial Role in Atherosclerosis Progression. To determine endothelial-specific Tie2-Cre activity, we detected fluorescence changes in cryosections of endothelium from carotid arteries of ROSA^{mTmG} and Tie2-Cre/ROSA^{mTmG} mice (*SI Appendix,* Fig. S1A). Semiquantitative RT-PCR revealed that significantly lower intimal *Pdcd5* mRNA levels in PDCD5cKO mice compared with wild-type (WT) mice. In contrast, *Pdcd5* mRNA levels in the media and adventitia showed no significant difference between PDCD5cKO and WT mice. Platelet endothelial cell adhesion molecule-1 (*Pecam-1*), the marker for endothelium, was present in the intima but not in the media and adventitia. In contrast, α-smooth muscle actin (*Sma*), the marker for smooth muscle cells, was not present in the intima. Quantitative RT-PCR showed that *Pdcd5* mRNA was rarely present in the intima of PDCD5cKO mice (*SI Appendix,* Fig. S1B). Body weight and electrocardiography findings were not different between the WT and PDCD5cKO mice (*SI Appendix,* Fig. S1 *C and D*). Furthermore, we did not find structural abnormalities, and the fluorescence intensities of PECAM-1–stained endothelium were not different between WT and PDCD5cKO lung, heart, or liver (*SI Appendix,* Fig. S2 *A and B*).

We adapted a partial carotid ligation model to evaluate the role of PDCD5 in endothelial dysfunction (18, 19). At 6 wk after left carotid partial ligation and initiation of a Paigen diet, neointima formation and luminal narrowing were significantly reduced in the PDCD5cKO mice (Fig. 1C). DAB (3,3′-diaminobenzidine) immunohistochemistry with SMA antibody showed significantly proliferated media and neointima in the ligated arteries of the WT mice, but not in those of the PDCD5cKO mice (Fig. 1B). Given the inhibited neointima proliferation in the PDCD5cKO mice, we assumed that PDCD5 expression of ECs could regulate the proliferation of VSMCs. After PDCD5 knockdown by siRNA in human umbilical vein endothelial cells (HUVECs), we cocultured HUVECs and human aorta VSMCs (HA-VMSCs) using 0.4-μm pore coculture dishes. We found that the proliferation of HA-VSMCs was significantly inhibited by PDCD5 knockdown in HUVECs (*SI Appendix,* Fig. S3A). Furthermore, PDCD5 knockdown elevated NO production in HUVECs as measured by 4-amino-5-methylamino-2′,7′-difluorofluorescein diacetate (DAF-FM DA) fluorescence density (*SI Appendix,* Fig. S3B). Immunofluorescence staining for PDCD5, phosphor-AKT, and PECAM-1 showed that PDCD5 was elevated in endothelium of ligated arteries, whereas phosphor-AKT was not elevated in WT mice. In contrast, both ligated and unligated arteries of PDCD5cKO mice showed significantly elevated phosphor-AKT expression in endothelium compared with WT mice (Fig. 1B). Moreover, fluorescence intensity profiles showed increased intensity of phosphor-AKT in endothelium of PDCD5cKO mice (Fig. 1C). Collectively, these results indicate that endothelial PDCD5 plays a crucial role in vascular homeostasis.

PDCD5 Antagonizes AKT-eNOS Signaling by Inhibiting HDAC3-AKT Interaction. We previously showed that PDCD5 binds to and inhibits HDAC3 function (20). Therefore, we next examined the molecular basis of PDCD5 involvement in AKT signaling. Consistent with a recent report (21), we also observed a selective interaction between AKT and HDAC3 among class I HDACs (*SI Appendix,* Fig. S4 *A and B*). Immunoprecipitation in HUVECs confirmed the endogenous interaction between HDAC3 and AKT (*SI Appendix,* Fig. S4C). We also verified the direct interaction between HDAC3 and AKT by a glutathione S-transferase pulldown assay (*SI Appendix,* Fig. S4D). Because PDCD5 was found to directly interact with HDAC3, we assumed that PDCD5 could regulate the HDAC3-AKT interaction. Immunoprecipitation assays revealed that overexpression of Flag-tagged PDCD5^{WT} significantly reduced the HDAC3–AKT interaction, whereas an HDAC3 binding-deficient mutant (20), Flag-tagged PDCD5^{L6R}, did not (Fig. 2A). An in vitro competition assay demonstrated that WT PDCD5, but not mutant PDCD5^{L6R}, competitively inhibited AKT binding to HDAC3 (*SI Appendix,* Fig. S4E). In situ proximity ligation assays (PLAs) to verify that PDCD5 overexpression in HUVECs
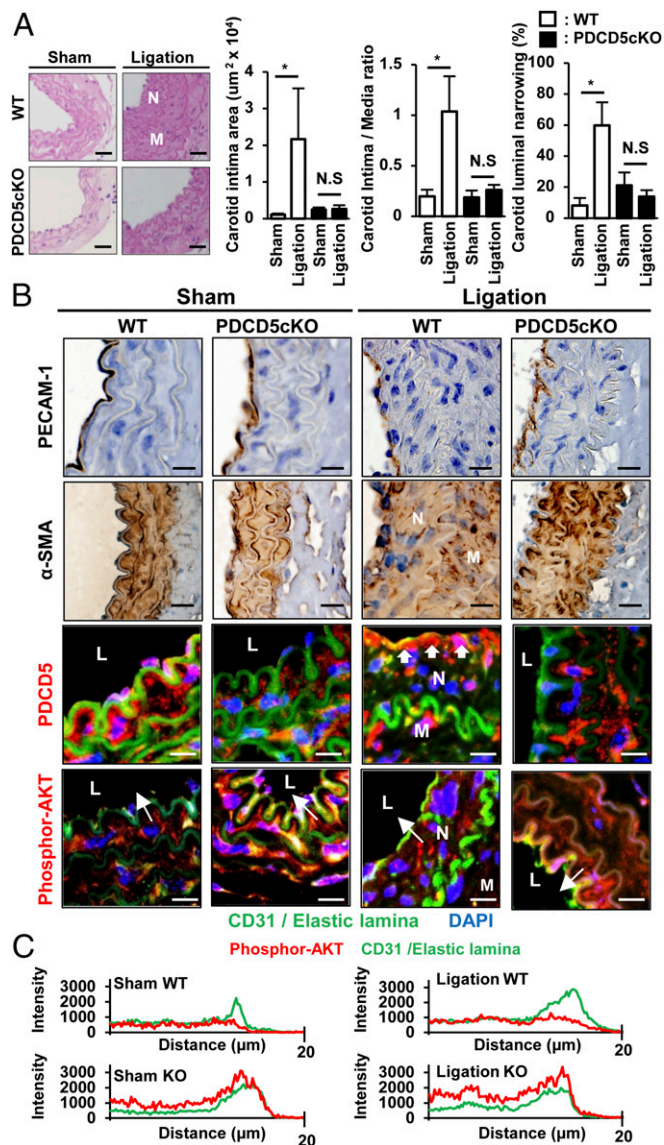
changes the HDAC3–AKT interaction revealed that 48 h after transfection with the overexpression vector, Flag-tagged PDCD5^{WT} overexpression effectively abolished the endogenous HDAC3–AKT interaction, whereas Flag-tagged PDCD5^{L6R} overexpression failed to inhibit the interaction with VEGF treatment (Fig. 2B). These results suggest that PDCD5 inhibits the interaction between HDAC3 and AKT.

We further examined the PDCD5 functions in AKT signaling using PDCD5 mutants. At 30 min after VEGF treatment, PDCD5^{WT}

Fig. 1. PDCD5 plays a crucial role in atherosclerosis progression. (*A*) Representative micrographs of an H&E-stained carotid lesion at 6 wk after partial ligation with a Paigen diet, showing the increase in media thickness and neoinitma formation. (Scale bars: 50 μm.) The intima area, luminal area, and intima/media ratio of partially ligated carotid arteries were quantified using ImageJ software. Error bars indicate SD (*n* = 4). Sham, the sham surgery group; ligation, the ligation surgery group. (*B*) Representative images showing fluorescence staining of PDCD5 (red), phosphor-AKT (red), and PECAM-1 (green) and DAB immunostaining of PECAM-1 and SMA in carotid lesions of WT and PDCD5cKO mice at 6 wk after partial ligation and a Paigen diet. Internal elastic lamina autofluorescence is shown in green, and the vascular lumen border is indicated by white broad arrows. (Scale bars: 20 μm.) In *A* and *B*, L indicates vascular lumen; M, media; N, neointima. N.S., not significant (*P* > 0.05); **P* < 0.05. (*C*) Micrographs were analyzed for intensity profile along the line drawn in white narrow arrows.
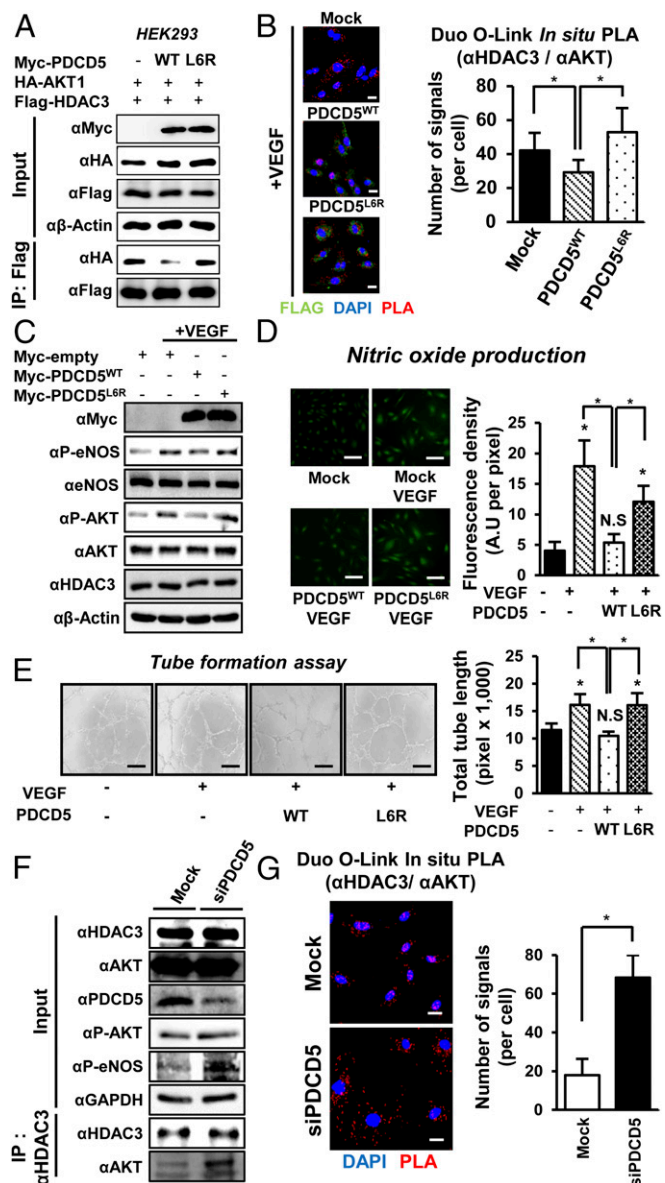
Fig. 2. PDCD5 antagonizes AKT-eNOS signaling by inhibiting the HDAC3–AKT interaction. (*A*) PDCD5 overexpression reduces the interaction between HDAC3 and AKT. HEK293 cells were transfected with Myc-tagged PDCD5^{WT}, Myc-tagged PDCD5^{L6R}, HA-tagged AKT1, and Flag-tagged HDAC3. Total cell extracts were immunoprecipitated with the Flag antibody. (*B*) In situ PLAs showing changes in the endogenous HDAC3–AKT interaction from mock, Flag-tagged PDCD5^{WT}, and Flag-tagged PDCD5^{L6R} overexpression in HUVECs. The number of dots per cell was counted using ImageJ software. Error bars indicate SD (*n* = 21). (Scale bars: 20 μm.) (*C*) Cells were transfected with Myc-tagged PDCD5^{WT} or Myc-tagged PDCD5^{L6R} mutant and then treated with VEGF (10 ng/mL) for 60 min. (*D*) DAF-FM DA staining for the determination of intracellular NO production. Representative images of HUVECs in 60-mm dishes were obtained by fluorescence microscopy at 60 min after VEGF treatment. Quantification of the fluorescence density of each cell was determined using ImageJ software. Error bars indicate SD (*n* = 10). (Scale bars: 100 μm.) (*E*) Tube formation assay with PDCD5^{L6R} and PDCD5^{WT} overexpression with VEGF treatment (10 ng/mL). Error bars indicate SD (*n* = 3). (Scale bars: 400 μm.) (*F* and *G*) Changes in the endogenous HDAC3–AKT interaction caused by PDCD5 knockdown using siRNA in HUVECs. (*F*) Coimmunoprecipitation assays showing changes in the endogenous HDAC3–AKT interaction. HUVECs were harvested at 48 h after PDCD5 siRNA transfection, and total cell extracts were immunoprecipitated using HDAC3 antibody. (*G*) In situ PLA showing changes in the endogenous HDAC3–AKT interaction. The number of dots per cell was counted using ImageJ software. Error bars indicate SD (*n* = 8). (Scale bars: 20 μm.) In *A–G*, N.S. indicates not significant (*P* > 0.05); *P < 0.05.

overexpression efficiently abolished AKT and eNOS phosphorylation in HUVECs, whereas PDCD5^{L6R} overexpression did not (Fig. 2*C*). Furthermore, Flag-PDCD5^{WT} overexpression significantly inhibited NO production measured by DAF-FM DA fluorescence density, whereas Flag-tagged PDCD5^{L6R} overexpression did not (Fig. 2*D*). Tube formation assays revealed that compared with PDCD5^{L6R} overexpression, PDCD5^{WT} overexpression effectively blocked tube formation (Fig. 2*E*). Consistently, PDCD5 knockdown strongly promoted the HDAC3–AKT interaction in immunoprecipitation assays (Fig. 2*F*) and PLAs (Fig. 2*G*).

PDCD5 Is Required for Anti-VEGF–Mediated Endothelial Cell Dysfunction. Bevacizumab, an anti-VEGF monoclonal antibody, effectively blocks VEGF-dependent AKT phosphorylation (22) and NO production (23). We next tested the possibility whether PDCD5 is required for anti-VEGF action of bevacizumab. To do so, we treated ECs with bevacizumab to evaluate endothelial function in anti-VEGF conditions. A time-course experiment with bevacizumab showed that PDCD5 levels increased after 4 h, with the greatest induction occurring at 12 h. In addition, AKT and eNOS phosphorylation decreased over time (Fig. 3*A* and *SI Appendix,* Fig. S5*A*). In contrast, PDCD5 expression significantly decreased after VEGF treatment (10 ng/mL) for 60 min. However, VEGF treatment with MG132 restored PDCD5 expression (*SI Appendix,* Fig. S5*C*).

We previously reported that the ubiquitination of PDCD5 plays an important role in PDCD5 function (20, 24); therefore, we examined whether VEGF regulates the stability of PDCD5 by ubiquitination. Interestingly, ubiquitination of PDCD5 increased after VEGF treatment (*SI Appendix,* Fig. S5*D*). Importantly, PDCD5 knockdown abolished bevacizumab-induced reductions of AKT and eNOS phosphorylation (Fig. 3*B* and *SI Appendix,* Fig. S5*B*), as well as cell viability (*SI Appendix,* Fig. S5*E*), suggesting a critical role of PDCD5 in anti-VEGF signaling.

In tube formation and scratch assays, bevacizumab did not inhibit migration or the formation of capillary-like tube structures in HUVECs with PDCD5 knockdown (Fig. 3 *C* and *D* and *SI Appendix,* Fig. S6 *A* and *B*). Furthermore, bevacizumab failed to inhibit NO production in the absence of PDCD5 (Fig. 3*E* and *SI Appendix,* Fig. S6*C*). To determine whether changes in the cell cycle caused functional changes in PDCD5-knockdown HUVECs, we performed FACS with propidium iodide staining. We observed no significant changes on cell cycle analysis (*SI Appendix,* Fig. S6*D*). Immunoprecipitation assays and in situ PLAs showed a decreased HDAC3–AKT interaction after bevacizumab treatment (*SI Appendix,* Fig. S7 *A* and *B*). In aortic ring assays, the number of microvessels sprouting from aortic rings was not inhibited by bevacizumab in PDCD5cKO mice and was significantly higher in PDCD5cKO mice compared with WT mice. The restoration of PDCD5 into PDCD5cKO aortas recovered the action of bevacizumab, suggesting a critical role of PDCD5 in endothelial function and vessel formation (Fig. 3*F* and *SI Appendix,* Fig. S5*F*).

Inhibition of HDAC3 Suppresses AKT-eNOS Signaling. Here we found that PDCD5 inhibited VEGF signaling by dissociating HDAC3 from AKT. In addition, PDCD5 depletion further increased AKT-eNOS signaling and abrogated anti-VEGF signaling. Thus, we next examined whether inhibition of HDAC3 restores the anti-VEGF action of bevacizumab in the absence of PDCD5. To do so, we first assessed the effects of HDAC3-specific inhibition and HDAC3 knockdown by siRNA. In HUVECs, AKT and eNOS phosphorylation significantly decreased with increasing concentrations of HDAC3 inhibitor (0–10 μmol/L). Those changes were most notable at a concentration of 1 μmol/L (Fig. 4*A* and *SI Appendix,* Fig. S8*A*). In the presence of VEGF (10 ng/mL), HUVECs treated with siHDAC3 or HDAC3 inhibitor displayed decreased AKT and eNOS phosphorylation (Fig. 4*B* and *SI Appendix,* Fig. S8*B*) and NO production (Fig. 4*C*). In aortic ring assays, ablation of PDCD5 gene further increased vessel sprouting compared with WT mice. Consistently, bevacizumab failed to
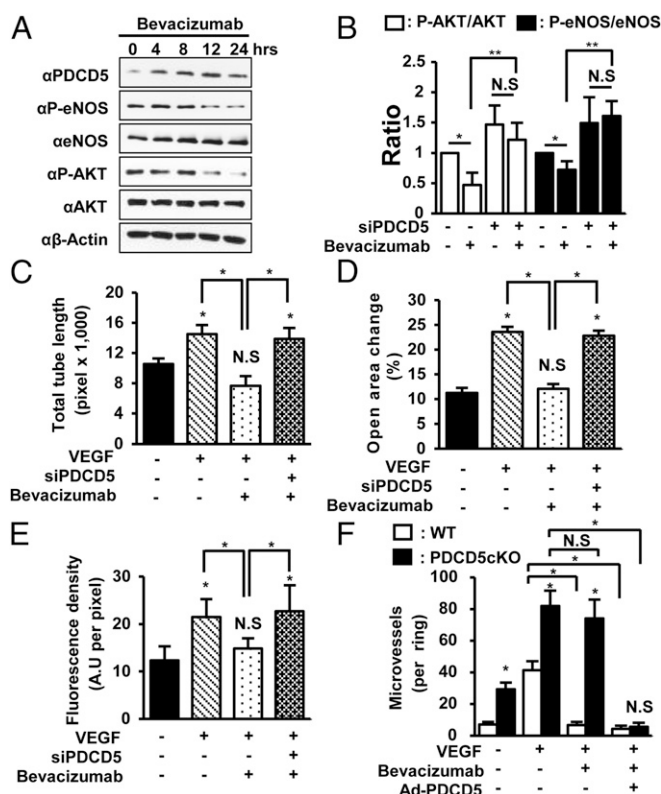
Fig. 3. PDCD5 is required for anti-VEGF–mediated EC dysfunction. (*A*) Representative immunoblot images of bevacizumab-treated HUVECs (1 mg/mL) at sequential time points over 24 h. (*B*) PDCD5 knockdown prevents bevacizumab-induced AKT and eNOS dephosphorylation. After 48 h of either mock or siPDCD5 siRNA transfection, HUVECs were treated with bevacizumab for 12 h. Immunoblots were quantified using ImageJ Software. Error bars indicate SD (*n* = 3). (*C–E*) The effects of PDCD5 knockdown in HUVECs were determined by tube formation (*C*), wound scratch (*D*), and NO production (*E*) assays. The images were quantified using ImageJ software. Error bars indicate SD (*n* = 10). (*F*) Each isolated carotid artery from WT and PDCD5cKO mice was embedded in Matrigel for microvessel sprouting in an aortic ring assay. Aortic rings were treated with VEGF (10 ng/mL) and bevacizumab (1 mg/mL). Aortic rings were also transduced with adenoviral vectors to rescue the expression of PDCD5 genes (Ad-PDCD5; 1 × 10^10 viral particles). Before being embedded in Matrigel, PDCD5 gene was transduced to the aortic ring by Ad-PDCD5 in serum-free medium for 24 h. Microvessel outgrowth was quantified by computerized image analysis. Error bars indicate SD (*n* = 3). In *A–F*, N.S. indicates not significant (*P* > 0.05); *P < 0.05.

reduce vessel sprouting in PDCD5cKO mice (Fig. 4*D*). Importantly, treatment of PDCD5cKO carotid arteries with HDAC3 inhibitor or shHDAC3 efficiently blocked vessel sprouting, verifying a crucial role of HDAC3 in AKT-eNOS signaling and NO production (Fig. 4 *D* and *E* and *SI Appendix*, Fig. S8 *C* and *D*). Consistent with HDAC3 inhibitor, treatment of AKT inhibitor inhibited vessel sprouting of aortas, as we expected (Fig. 4*E*).

Serum PDCD5 Reflects Cardiovascular Risks. It has been reported that PDCD5 protein is present in human serum. We next examined whether serum PDCD5 originates in ECs. We successfully detected PDCD5 protein in media containing HUVECs under serum-free conditions (Fig. 5*A*). Furthermore, bevacizumab treatment increased PDCD5 levels in a time-dependent manner in both ECs and the medium (Fig. 5*B*). Interestingly, rhPDCD5 enters cells via the shuttle system (25); therefore, we hypothesized that the administration of rhPDCD5 could mimic circumstances of PDCD5 up-regulation in the endothelium. HUVECs treated with increasing doses of rhPDCD5 (0–5 μg/mL) showed significantly reduced AKT and eNOS phosphorylation (Fig. 5*C*).

We next examined the significance of serum PDCD5 in cardiovascular disease. Serum nitrite/nitrate levels were significantly higher in PDCD5cKO mice compared with WT mice (Fig. 5*D*). In 86 randomly selected serum samples from the Cardiovascular and Metabolic Disease Etiology Research Center–High Risk (CMERC-HI) cohort, the results of Griess reactions revealed a significant negative correlation between log serum PDCD5 and log serum nitrite/nitrate levels (*r* = 0.284; *P* = 0.008).

Finally, we analyzed the correlation between serum PDCD5 and clinical cardiovascular risk factors in all 566 study participants. The baseline characteristics of the participants are presented in *SI Appendix*, Table S2. The log-transformed serum PDCD5 levels were statistically different between males and females and were correlated with hypertension, diabetes mellitus, left ventricular hypertrophy, coronary artery calcium score, and HDL cholesterol level (all *P* < 0.05; Fig. 5 *F* and *G* and *SI Appendix*, Fig. S9). Multivariate regression revealed that diabetes mellitus, HDL
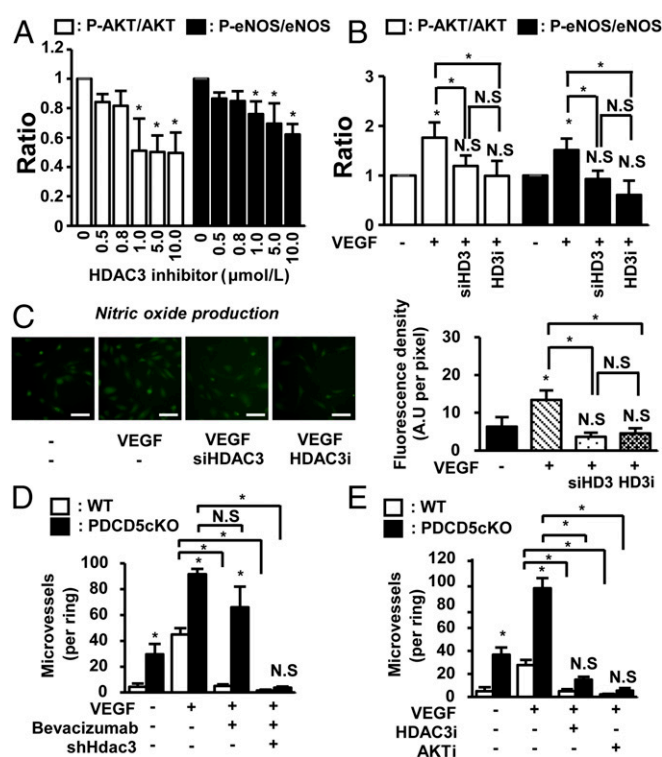

Fig. 4. Inhibition of HDAC3 suppresses AKT-eNOS signaling. (*A*) HUVECs were treated with increasing concentrations (0–10 μmol/L) of HDAC3 inhibitor for 24 h. Total lysates were immunoblotted with the indicated antibodies. Immunoblots were quantified using ImageJ software. Error bars indicate SD (*n* = 3). (*B* and *C*) HDAC3 inhibitor (1 μmol/L) or siHDAC3 was treated with HUVECs for 48 h, then the HUVECs were incubated with VEGF (10 ng/mL) for 60 min. Immunoblots were quantified using ImageJ software. Error bars indicate SD (*n* = 3). (*B*) Total lysates were immunoblotted with the indicated antibodies. (*C*) DAF-FM DA staining for the detection of intracellular NO production. Quantification of the fluorescence density of each cell was determined using ImageJ software. Error bars indicate SD (*n* = 7). (Scale bars: 100 μm.) (*D* and *E*) Each isolated carotid artery from WT and endothelial-specific PDCD5 knockout mice was embedded in Matrigel for microvessel sprouting in an aortic ring assay. Microvessel outgrowth was quantified by computerized image analysis. Error bars indicate SD (*n* = 4). (*D*) An aortic ring assay was performed with Hdac3-shRNA-GFP adenovirus (1 × 10^10 viral particles) and bevacizumab (1 mg/mL). Before being embedded in Matrigel, aortic rings were treated with Hdac3-shRNA-GFP adenovirus in serum-free medium for 24 h. (*E*) An aortic ring assay was performed with HDAC3 inhibitor (1 μmol/L) and AKT inhibitor (1 μmol/L). In *A–E*, N.S. indicates not significant (*P* > 0.05); *P < 0.05.
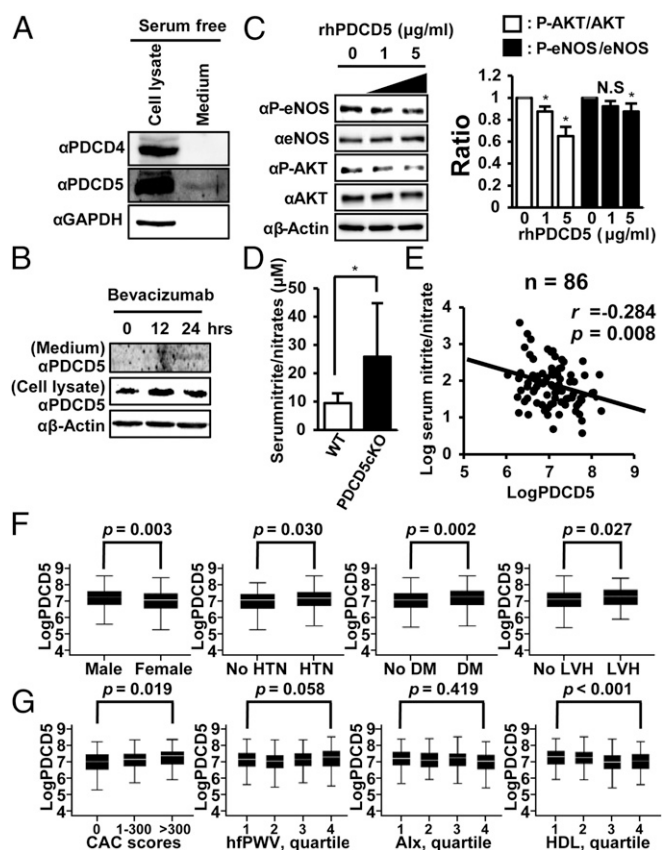
Fig. 5. Serum PDCD5 reflects cardiovascular risk. (A) HUVECs were cultured without serum and other growth factors for 24 h. Cells and medium were isolated by centrifugation, and the medium was concentrated by a 10 kDa-cutoff spin column. (B) HUVECs with complete medium were incubated with 1 mg/mL bevacizumab for the indicated times. Excess protein was removed from the media with a 30-kDa-cutoff spin column, and the media was then concentrated by a 10- kDa-cutoff spin column sequentially. (C) Exogenous recombinant human PDCD5 protein alone effectively inhibits AKT-eNOS signaling. (D) A Griess reaction to detect serum nitrite/nitrate was performed using 8-wk-old WT (n = 18) and PDCD5cKO mice (n = 9). Error bars indicate SD. (E–G) Human serum PDCD5 levels were measured by indirect double-sandwich ELISA. (E) Scatterplot of log serum PDCD5 and log serum nitrite/nitrate. A Griess reaction for detection of serum nitrite/nitrate was performed using the randomly selected serum samples from the CMERC-HI cohort (n = 86). Pearson's correlation coefficient, r, with P value was calculated for each sample. (F and G) Boxplots of log serum PDCD5. The horizontal line within the box indicates the median, the boundaries of the box indicate the 25th and 75th percentiles, and the whiskers indicate the highest and lowest values of the results. (F) Associations between log serum PDCD5 levels and clinical characteristics, including sex, hypertension (HTN), diabetes mellitus (DM), and left ventricular hypertrophy (LVH). (G) Associations between log serum PDCD5 levels and cardiovascular risk predictors, including coronary calcium (CAC) score, heart to femoral pulse wave velocity (hfPWV), augmentation index (AIx), and HDL cholesterol level. *P < 0.05.

cholesterol level, and coronary artery calcium score were representative of serum log PDCD5 (all *P* < 0.05; *SI Appendix*, Table S3).

Discussion

The vascular endothelium is a dynamic and multifunctional system. Changes in endothelial function contribute critically to atherosclerosis progression (26); therefore, a molecular and clinical assessment of the endothelium is very important. Our translational study provides evidence of PDCD5-dependent endothelial dysfunction through the AKT pathway. Elevated intracellular levels of PDCD5 dissociate the HDAC3–AKT interaction and inhibit NO production. In the absence of PDCD5, the HDAC3–AKT

interaction was increased and the anti-VEGF action of bevacizumab was abolished in HUVECs and mice aortas, highlighting the critical role of PDCD5 in AKT-eNOS signaling through HDAC3. Furthermore, the serum PDCD5 level reflects atherosclerosis severity and NO production in humans. rhPDCD5 effectively interrupted AKT signaling. Collectively, our findings delineate a role of PDCD5 in endothelial dysfunction and atherosclerosis progression (*SI Appendix*, Fig. S10).

PDCD5 is a small, 14-kDa protein induced during apoptosis (4, 20, 27). It is generally down-regulated in various cancers, and the inhibition of PDCD5 blocks apoptosis. Structurally, PDCD5 has a rigid core region and two dissociated terminal regions. The N-terminal 26-residue fragment of PDCD5 forms a stable α-helical structure. PDCD5 lacking the N-terminal structure does not induce apoptosis in HL-60 cells (28). We previously reported that HDAC3 interacts with PDCD5, and the PDCD5^{L6R} mutant, which has a defective interaction with HDAC3, did not alter HDAC3 activity (20). Because the alpha-helix structure can effectively inhibit protein–protein interaction (29), we hypothesized that the N terminus of PDCD5 has a central role in protein–protein interaction as well as PDCD5 stability, and thus might perform various functions. Otherwise, the C-terminal residues 109–115 of PDCD5 represent an important region for rhPDCD5 internalization, which increases the extent of apoptosis (25, 30). The clathrin-independent endocytic pathways participate in rhPDCD5 internalization, and the exact mechanism depends on the cell. Although various studies of rhPDCD5 have been performed, the significance of serum PDCD5 has not been fully elucidated until now. More importantly, the interesting question of how the PDCD5 protein is secreted by a cell has been unanswered.

In this study, we found that serum PDCD5 levels reflect vascular conditions, including NO production, and are significantly correlated with diabetes mellitus, HDL cholesterol level, and coronary calcium score. Diabetes mellitus is a major risk factor for cardiovascular disease and endothelial function (31). A previous study reported that HDL cholesterol alone can activate the AKT-eNOS pathway (32). Although whether the coronary calcium score is correlated with estimated endothelial dysfunction is controversial (33, 34), it is evident that coronary calcium level reflects the risk of cardiovascular disease (35, 36). Therefore, our results suggest that PDCD5 is associated with endothelial dysfunction and cardiovascular disease. Because the CMERC-HI is a prospective cohort study, further analysis of the correlation between serum PDCD5 and cardiovascular outcomes is needed. We found that exogenous PDCD5 protein significantly inhibited endothelial AKT phosphorylation and NO synthesis in HUVECs. Thus, PDCD5 protein present in the serum might also induce endothelial dysfunction, and further evaluation is needed to determine whether serum PDCD5 enters and affects ECs in an animal model.

We have identified some hitherto unreported intracellular functions of PDCD5. When endothelial dysfunction is induced in the presence of anti-VEGF, intracellular levels of PDCD5 are increased, leading to collapse of the HDAC3–AKT interaction. Thus, AKT signaling through HDAC3 is degraded, which may interfere with the maintenance of endothelial integrity. In contrast, ubiquitination of PDCD5 is increased with VEGF, and it enhances HDAC3-AKT signaling. In other words, PDCD5 is an endogenous regulator of HDAC3, meaning that it can become a new molecular target in endothelial-mediated disease.

Several studies have reported that global HDAC inhibitors, such as trichostatin A, can prevent the progression of atherosclerosis (37, 38). In contrast, several groups have found that HDAC inhibitors may stimulate atherogenesis (39). Those discrepancies are due to the use of pan-HDAC inhibitors and various microvascular components, such as intima, media, and adventitia. Furthermore, HDAC function also depends on interactions with various cytokines and immune cells in the blood. To overcome the limitations of previous studies, one study has used specific HDAC inhibitors, and further studies using a conditional KO mouse system are needed. A recent study showed

that HDAC3 decreased Lys-20 acetylation and increased S473 phosphorylation of AKT (21). That study also revealed that HDAC3-specific inhibitor suppressed the HDAC3–AKT interaction. In our study, the use of an HDAC3-specific inhibitor reduced AKT and eNOS phosphorylation and NO production in ECs. We also performed aortic ring assays to exclude the effects of extravascular components, such as immune cells and cytokines, and those assays produced results similar to those of our in vitro experiments. Nevertheless, the possibility of interaction between ECs and VSMCs remains, and the possibility of unintended effects of other types of HDACs cannot be completely ruled out. Therefore, further studies of the functions of other HDACs and microenvironments, including smooth muscle cells, are needed.

Taken together, our results reveal that PDCD5 negatively regulates AKT signaling through HDAC3 and has clinical implications in the endothelium. Our results strongly suggest that PDCD5 can be a useful therapeutic target in cardiovascular disease.

Materials and Methods

1. Davignon J, Ganz P (2004) Role of endothelial dysfunction in atherosclerosis. *Circulation* 109(23, Suppl 1):III27–III32.
2. Kawashima S, Yokoyama M (2004) Dysfunction of endothelial nitric oxide synthase and atherosclerosis. *Arterioscler Thromb Vasc Biol* 24:998–1005.
3. Liu H, et al. (1999) TFAR19, a novel apoptosis-related gene cloned from human leukemia cell line TF-1, could enhance apoptosis of some tumor cells induced by growth factor withdrawal. *Biochem Biophys Res Commun* 254:203–210.
4. Xu L, et al. (2012) PDCD5 interacts with p53 and functions as a positive regulator in the p53 pathway. *Apoptosis* 17:1235–1245.
5. Wang Y, et al. (2004) An alternative form of paraptosis-like cell death, triggered by TAJ/TROY and enhanced by PDCD5 overexpression. *J Cell Sci* 117:1525–1532.
6. Jiang Z, et al. (2014) Autophagic effect of programmed cell death 5 (PDCD5) after focal cerebral ischemic reperfusion injury in rats. *Neurosci Lett* 566:298–303.
7. An L, et al. (2012) Involvement of autophagy in cardiac remodeling in transgenic mice with cardiac specific over-expression of human programmed cell death 5. *PLoS One* 7: e30097.
8. Fu DZ, Cheng Y, He H, Liu HY, Liu YF (2013) PDCD5 expression predicts a favorable outcome in patients with hepatocellular carcinoma. *Int J Oncol* 43:821–830.
9. Spinola M, et al. (2006) Association of the PDCD5 locus with lung cancer risk and prognosis in smokers. *J Clin Oncol* 24:1672–1678.
10. Hedenfalk I, et al. (2001) Gene-expression profiles in hereditary breast cancer. *N Engl J Med* 344:539–548.
11. Chen CH, et al. (2013) The involvement of programmed cell death 5 (PDCD5) in the regulation of apoptosis in cerebral ischemia/reperfusion injury. *CNS Neurosci Ther* 19: 566–576.
12. Wang J, Guan Z, Ge Z (2013) Plasma and synovial fluid programmed cell death 5 (PDCD5) levels are inversely associated with TNF-α and disease activity in patients with rheumatoid arthritis. *Biomarkers* 18:155–159.
13. Chen Y, et al. (2013) Serum programmed cell death protein 5 (PDCD5) levels is upregulated in liver diseases. *J Immunoassay Immunochem* 34:294–304.
14. Longworth MS, Laimins LA (2006) Histone deacetylase 3 localizes to the plasma membrane and is a substrate of Src. *Oncogene* 25:4495–4500.
15. Bhaskara S, et al. (2010) Hdac3 is essential for the maintenance of chromatin structure and genome stability. *Cancer Cell* 18:436–447.
16. Yao YL, Yang WM (2011) Beyond histone and deacetylase: An overview of cytoplasmic histone deacetylases and their nonhistone substrates. *J Biomed Biotechnol* 2011:146493.
17. Zampetaki A, et al. (2010) Histone deacetylase 3 is critical in endothelial survival and atherosclerosis development in response to disturbed flow. *Circulation* 121:132–142.
18. Nam D, et al. (2009) Partial carotid ligation is a model of acutely induced disturbed flow, leading to rapid endothelial dysfunction and atherosclerosis. *Am J Physiol Heart Circ Physiol* 297:H1535–H1543.
19. Korshunov VA, Berk BC (2003) Flow-induced vascular remodeling in the mouse: A model for carotid intima-media thickening. *Arterioscler Thromb Vasc Biol* 23: 2185–2191.
20. Choi HK, et al. (2015) Programmed cell death 5 mediates HDAC3 decay to promote genotoxic stress response. *Nat Commun* 6:7390, and erratum (2015) 6:8225.
21. Long J, et al. (2017) Targeting HDAC3, a new partner protein of AKT in the reversal of chemoresistance in acute myeloid leukemia via DNA damage response. *Leukemia* 31: 2761–2770.
22. Shin SJ, et al. (2013) Circulating vascular endothelial growth factor receptor 2/pAkt-positive cells as a functional pharmacodynamic marker in metastatic colorectal cancers treated with antiangiogenic agent. *Invest New Drugs* 31:1–13.
23. Dinc E, Yildirim O, Ayaz L, Ozcan T, Yilmaz SN (2015) Effects of intravitreal injection of bevacizumab on nitric oxide levels. *Eye (Lond)* 29:436–442.
24. Park SY, et al. (2015) Deubiquitinase OTUD5 mediates the sequential activation of PDCD5 and p53 in response to genotoxic stress. *Cancer Lett* 357:419–427.
25. Wang Y, et al. (2006) Cellular uptake of exogenous human PDCD5 protein. *J Biol Chem* 281:24803–24817.
26. Deanfield JE, Halcox JP, Rabelink TJ (2007) Endothelial function and dysfunction: Testing and clinical relevance. *Circulation* 115:1285–1295.
27. Xu HY, et al. (2012) Transfection of PDCD5 effect on the biological behavior of tumor cells and sensitized gastric cancer cells to cisplatin-induced apoptosis. *Dig Dis Sci* 57: 1847–1856.
28. Liu D, et al. (2005) The N-terminal 26-residue fragment of human programmed cell death 5 protein can form a stable alpha-helix having unique electrostatic potential character. *Biochem J* 392:47–54.
29. Azzarito V, Long K, Murphy NS, Wilson AJ (2013) Inhibition of α-helix-mediated protein-protein interactions using designed molecules. *Nat Chem* 5:161–173.
30. Fu DZ, Cheng Y, He H, Liu HY, Liu YF (2015) Recombinant human PDCD5 exhibits an antitumor role in hepatocellular carcinoma cells via clathrin-dependent endocytosis. *Mol Med Rep* 12:8135–8140.
31. Tabit CE, Chung WB, Hamburg NM, Vita JA (2010) Endothelial dysfunction in diabetes mellitus: Molecular mechanisms and clinical implications. *Rev Endocr Metab Disord* 11:61–74.
32. Mineo C, Yuhanna IS, Quon MJ, Shaul PW (2003) High-density lipoprotein-induced endothelial nitric oxide synthase activation is mediated by Akt and MAP kinases. *J Biol Chem* 278:9142–9149.
33. Ramadan MM, et al. (2008) Evaluation of coronary calcium score by multidetector computed tomography in relation to endothelial function and inflammatory markers in asymptomatic individuals. *Circ J* 72:778–785.
34. Kullo IJ, et al. (2007) Brachial artery diameter and vasodilator response to nitroglycerine, but not flow-mediated dilatation, are associated with the presence and quantity of coronary artery calcium in asymptomatic adults. *Clin Sci (Lond)* 112: 175–182.
35. Raggi P, et al. (2008) Coronary artery calcium to predict all-cause mortality in elderly men and women. *J Am Coll Cardiol* 52:17–23.
36. Budoff MJ, et al. (2007) Long-term prognosis associated with coronary calcification: Observations from a registry of 25,253 patients. *J Am Coll Cardiol* 49:1860–1870.
37. Kee HJ, et al. (2011) Trichostatin A prevents neointimal hyperplasia via activation of Krüppel like factor 4. *Vascul Pharmacol* 55:127–134.
38. Okamoto H, et al. (2006) Trichostatin A, an inhibitor of histone deacetylase, inhibits smooth muscle cell proliferation via induction of p21(WAF1). *J Atheroscler Thromb* 13:183–191.
39. Choi JH, et al. (2005) Trichostatin A exacerbates atherosclerosis in low-density lipoprotein receptor-deficient mice. *Arterioscler Thromb Vasc Biol* 25:2404–2409.